Available online at www.sciencedirect.com
SCIENCE DIRECT®
Composites Science and Technology 64 (2004) 2067–2074
COMPOSITES SCIENCE AND TECHNOLOGY
www.elsevier.com/locate/compscitech

Effect of gas pressure infiltration on microstructure and bending strength of porous Al_2O_3/SiC-reinforced aluminium matrix composites

Adem Demir *, Necat Altinkok

Department of Metal Education, Technical Education Faculty, Sakarya University, Esentepe, 54187 Sakarya, Turkey

Received 7 October 2003; received in revised form 14 December 2003; accepted 25 February 2004
Available online 1 June 2004

Abstract

High porous ceramic preforms were produced by chemical route, and molten aluminium was infiltrated into these preforms by using gas pressure. Slurry was prepared by mixing aluminium sulphate and ammonium sulphate in the water, and silicon carbide powder was added into the slurry. The slurry was heated up in a ceramic crucible in the open air furnace up to 1200 °C to fabricate dual ceramic preform. At the end of the reaction sequences, 3D honeycomb structure α-alumina grains and uniformly distributed SiC cake were obtained. An apparatus was designed for gas pressure infiltration of Al alloys into the preform. The preforms which contained different amount of porosity were infiltrated with different pressures and temperatures. Not only porosity but also pore size affects infiltration rate. The resulting preforms and metal-matrix composites were characterised by optical and SEM observations. Three point bending tests were applied for the infiltrated metal-matrix composites (MMCs). The highest strength value (558 MPa) was obtained at 800 °C and 3 MPa. By controlling fabrication procedure of Al_2O_3/SiC preforms and infiltration conditions, this high strength in the composite is obtained. The networking flaky alumina particles and encapsulated SiC particles within the preform delayed crack propagation and provided crack deflection during the fracture.

Keywords: Preform preparation; A. Metal-matrix composites

1. Introduction

Recently, the demands for lightweight materials having high strength and high stiffness have attracted much interest in the development of the fabrication processes for metal-matrix composites (MMCs). The most important limitation on the production of MMCs by liquid-phase process resides upon the compatibility of the reinforcement and the matrix [1]. This problem is especially important in the case of aluminium matrix composites, for aluminium is usually covered with a thin oxide layer which blocks surface wetting and reacts with some ceramics to form intermetallics which will influence the final properties of the composites. Several methods were investigated to improve the compatibility of matrix and reinforcement interface, and of these the squeeze-casting process was the most suitable. Since contact duration between the reinforcement and the matrix was short, the interface reactions were decreased to improve wettabillity.

Particulate-reinforced composites are economically cheaper in view of raw materials and fabrication processes, and have potential for applications requiring relatively large volume production. The ease of MMCs' fabrication is also another favourable factor. These can be produced by (powder metallurgy) liquid metallurgy or metal spray methods. All such processes are readily available for manufacturing unreinforced alloys. In addition, the use of a secondary process, such as rolling, forging, extrusion and heat treatment, can be applied only to discontinuously reinforced composite without incurring significant damage to the reinforcement [2]. The infiltration of ceramic preforms is a common route

* Corresponding author.
E-mail address: ademir@sakarya.edu.tr (A. Demir).

0266-3538/$ - see front matter © 2004 Elsevier Ltd. All rights reserved.
doi:10.1016/j.compscitech.2004.02.015

to produce MMCs. In particular, squeeze casting provides good infiltration quality of chopped preforms [3–6]. This procedure consists of pushing the molten metal into a preheated preform using a piston and pressures in the range of 50–100 MPa. Despite the good results obtained with this technique, some difficulties remain related with air entrapment into the preform [7,8] which can be at the origin of voids at metal ceramic interfaces. These deteriorate the mechanical properties of preform. An additional problem is related to the high pressure involved in the process, which implies the development of heavy equipment even for laboratory research. Moreover, high pressure could produce fibre damage or an inhomogeneous fibre distribution along the infiltration direction [5].

In order to solve these problems, low pressure infiltration processes have been developed [9–12]. Compared to squeeze casting, the infiltration pressure can be substantially reduced if the vacuum is made in the preform to avoid air entrapment [13]. Consequently, relatively low-cost production method can be developed by using a gas pressure to achieve infiltration. In this work, a gas pressure infiltration apparatus has been developed for MMCs processing at the laboratory condition. This apparatus is based on the idea that alloy melting and preform infiltration should be done in different chambers. Consequently, the apparatus is divided into two parts: a melting chamber, where the alloy is melted under protective or vacuum atmosphere, and an infiltration chamber, where the molten metal is pushed into the preform by gas pressure. The resulting preforms and infiltrated composites have been physically and mechanically characterised.

2. Experimental

Al_2O_3/SiC particles reinforced in aluminium matrix composites were produced by using preforms and gas pressure infiltration system, which was developed especially for this study. Aluminium sulphate $Al_2(SO_4)_3 \cdot xH_2O$ ($x = 14$–16), ammonium sulphate $(NH_4)_2SO_4$, water and silicon carbide particles (3–10 μm) were mixed within a ceramic crucible and reacted in a muffle furnace at 1200 °C for 2 h. When the sulphates were dissolved in water, the solution consisted of $(NH_4)_2SO_4$ (132 g/mol), $Al_2(SO_4)_3 \cdot 24H_2O$ (342 g/mol) and SiC particles before reaction. As the temperature increased, the aqueous solution started to boil and foam with evaporation of excess water. At the end of this reaction, ammonium alum $(NH_4)_2\ SO_4 \cdot Al_2(SO_4)_3$ was obtained. With increasing temperature, ammonium alum started to decompose causing ammonia and residual water loss. In the final decomposition, sulphate ions were volatilised and high porous alumina cake left at 900 °C. At this point, decomposition was completed but δ to α-Al_2O_3 transformation was not completed according to Pacewsca [14]. Therefore, the temperature was increased up to 1200 °C and held for 2 h so that the thermal transformation of the transition alumina into α-alumina could be completed. At the end of these reaction sequences, highly porous (up to 95 vol%) alumina containing SiCp ceramic composite preform was obtained.

An infiltration apparatus which was designed in previous study [15] was to melt and infiltrate aluminium alloys into the preform. The resulting preforms were cut and placed into the infiltration chamber, which was located in the lower section of the device. Al–Si alloy (containing 10% Si and 1.2% Mg), supplied from 3A Aluminium-Turkey, was put into the plasma-coated stainless steel crucible, which was located in the upper section of the device. After the preform and Al alloy positioned, the system was closed. Before heating, air in the system was swept out by argon gas and then the gas flow was stopped and the system was vacuumed. The crucible was heated to above the melting point of the alloy and the die was heated at about 550 °C. Melting was carried out under horizontal position to prevent liquid Al leak until the temperature reached infiltration temperatures, then the system positioned vertically. When the temperature reached the infiltration temperature, the gas was released to push down the liquid aluminium. Gas pressure 1–3 (MPa) was increasingly applied to obtain successful production of Al_2O_3/SiC-reinforced Al matrix composites. The applied pressure is held constant until solidification was completed and the remaining melt was used to feed the solidification shrinkage. Three point bend tests were performed on a DARTEC mechanical testing machine. The samples for the tests were of 40 mm length × 6.35 mm height × 12.7 mm width with the specimen height parallel to the press force direction [16]. The span of the two sustaining points was 25.4 mm. SEM image analysis and EDS element analysis of the polished and fracture surfaces of the composites and preforms were carried out on a CamScan S4 scanning electron microscope. Porosity and density measurement were carried out by Archimedes' principle. Pore size, distribution and alumina/SiC grain size and shape were determined with SEM image analysis.

3. Results and discussion

3.1. Microstructures and properties of composites

For metal infiltration, high porous preform preparation is essential. Porosity and mean pore size are important variables affecting infiltration rate. Over 75 vol% porosity and larger pore size (over 20 μm) are the key points of successful infiltration. The method of alumina production from aluminium sulphate was pro-

vided such ceramic preform. High porous α-alumina was obtained from decomposition of aluminium sulphate (87 wt%) and ammonium sulphate (13 wt%) aqueous solution after firing at 1200 °C as shown in Fig. 1(a). Detailed reactions of the preform preparation were explained elsewhere [15]. X-ray analysis showed that corundum α-alumina was obtained after decomposition of aluminium sulphate. Addition of SiC particles to the solution before firing also resulted in high porous alumina/SiC mix cake as shown in Fig. 1(b), but the porosity and pore size changed according to SiC addition and SiC particle sizes. The resulting preform looks like 3D honeycomb structures with the flaky alumina grains surrounding SiC particles. This structure is quite ideal for liquid metal infiltration, since most of the preforms have over 75 vol% of porosity. Since SiC particles are uniformly dispersed in viscous solution during foaming, they are encapsulated by alumina ceramic after alumina formation. This is a unique structure that cannot be obtained by conventional powder processing.

The water-free starting composition and resulting Al_2O_3/SiC ceramic mix cakes after firing are shown in Table 1. To achieve this reaction, the composition was dissolved in water which was equal to weight in aluminium sulphate. As shown in Table 1, SiC particles are increasingly added to the aqueous solution to adjust alumina/SiC ratio and porosity. It is possible to control porosity by changing the alumina/SiC ratio in the cake. Since the method of alumina production results in ceramic composite network, decreasing the alumina fraction leads to less volume fraction of porosity. When 87 wt% aluminium sulphate and 13 wt% ammonium sulphate were reacted at 1200 °C, the resulting alumina was 16 wt% of aluminium sulphate. When monolithic alumina is produced from the firing of aluminium sulphate and ammonium sulphate aqueous solution, highly porous alumina cake (up to 95 vol%) can be produced. If the SiC particles are added into the aqueous solution before firing, less porous alumina/SiC cakes can also be produced. The lower foaming was observed as higher SiC particle size and amount of particle were used. Since the foamed structure turned to α-alumina in the final stage, the foaming characteristics turned preform characteristics. Hence, the rate-controlling mechanism for porosity was alumina ratio and its grain growth during preform fabrication. Therefore, SiC addition was provided at different ratios of Al_2O_3/SiC cake and porosity

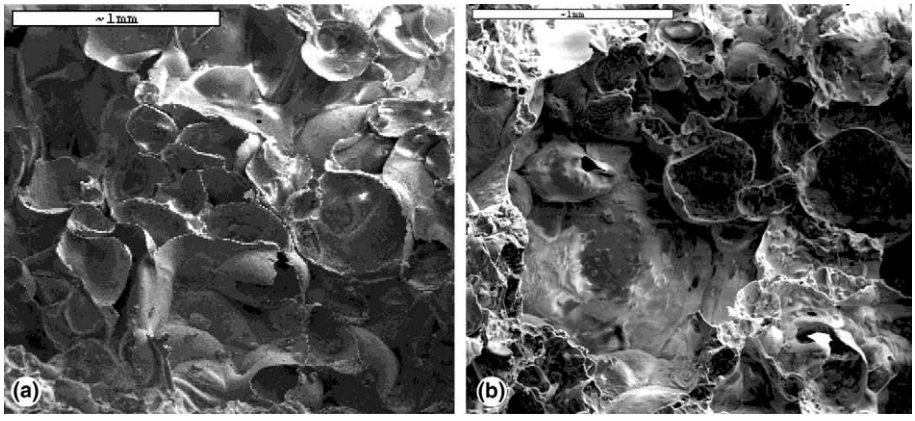

Fig. 1. SEM images of porous ceramic preforms: (a) 100% alumina and (b) 50% Al_2O_3 and 50% SiC ceramic cake.

Table 1
Starting compositions and firing products for different Al_2O_3/SiC ceramic cakes

Starting compositions before water addition				Al_2O_3/SiC cake after firing at 1200 °C	
Samples	$Al_2(SO_4)_3 \cdot xH_2O$ (wt%)	$(NH_4)_2SO_4$ (wt%)	SiC (wt%)	SiC wt% in cake	Porosity (vol%)
C05	85.47	12.82	1.71	12	95
C06	84.03	12.61	3.36	20	94
C07	82.03	12.31	5.66	30	93
C13	76.33	11.45	12.21	50	87
C21	71.94	10.79	17.27	60	79
C32	65.79	9.87	24.34	70	68
C37	61.35	9.20	29.44	75	63
C41	55.86	8.38	35.75	80	59
C45	38.61	5.79	55.60	90	55

in the range from 55 to 95 vol%, which provided different range of particle reinforcement from 45 to 5 vol% named as C45 and C05 for samples, respectively.

The porous ceramic preforms were placed into the infiltration chamber and liquid aluminium alloy was infiltrated with this Al–Si alloy at different temperatures and pressures. As shown in Table 2, infiltration temperature and pressure are both effective to achieve full infiltration. Because wettability of liquid aluminium to Al_2O_3 is poor, gas pressure is needed to infiltrate aluminium into the whole preform. As the temperature and pressure are increased, the degree of infiltration is also increased. The shape of the infiltration front strongly depends on whether viscous or capillary forces dominate. If capillary forces dominate, the infiltration process is adequately described by means of a model called invasion percolation described by Garcia-Cordovilla et al. [10]. If the applied pressure P is higher than atmospheric pressure P_0 but smaller than a critical pressure P_c, the front will be rough in the non-wetting case. Increasing P gradually reduces the roughness of the front. On the other hand, for contact angles below a critical value of 45°, partial wetting occurs and the fluid floods the system uniformly, leading to a low porosity and a rather flat infiltration front. As the temperature rises, the viscosity of the liquid decreases, and because of lower viscosity, it is possible to obtain better infiltration but it is not possible to achieve full infiltration without pressure. In the mean time, pressure itself is not sufficient to achieve full infiltration at lower temperatures. At higher temperatures high pressure is not necessary to get full density but higher temperatures result in grain coarsening of the matrix. Hence, at 800 °C infiltration temperature and 3 MPa pressures were determined as an optimum condition to achieve full infiltration in spite of large dendrites.

As the temperature and pressure increase, the relative densities of the samples approach theoretical density (TD) as shown in Fig. 2. As the infiltration temperature increases, three different relative density curves were observed for three different gas pressures. At 1 MPa constant applied pressure, relative density can be increased from 63.5% to 96.5% by changing the temperature from 650 to 800 °C, respectively. When the pressure increased by 3 MPa, 80.9% of TD can be obtained even at lowest temperature (650 °C). This shows that pressure increase is very effective at low infiltration temperatures. On the other hand, the temperature is very effective at high infiltration temperatures. This means that if infiltration is carried out at low temperatures, high pressure is needed. However, if it is carried out at high temperatures, low pressure is enough to achieve full densification. Therefore, as shown in Fig. 2, density differences at low temperature are much higher than that of high infiltration temperatures. Since wetting of aluminium-alumina is poor, silicon and magnesium containing Al alloy was used to increase wetting properties and to decrease viscosity. Silicon is widely used alloying element in aluminium alloys since it gives higher strength. Silicon additions to aluminium alloys positively affect the alloy's fluidity and reduce its melting temperature. Mg also reduces the surface tension and the contact angle between Al and SiC, and thus their presence in the alloy is essential in infiltrating ceramic preforms with aluminium alloys. The porosity and pore size are also important to achieve full densification. As a result of high porosity and large open pores of the in-house preform, the liquid Al–Si–Mg alloy can easily be infiltrated to the fine pores when high temperature and pressure are applied. The main properties of the preform are inter-connection of large and small pores allowing easy melt penetration because of low surface tension resulting from large disintegration of the liquid. If the preform contains fine pores throughout the composite, it is difficult to overcome threshold pressure due to the high surface tension. Another drawback of small pore is

Table 2
Effect of infiltration temperature and pressure on composite properties for sample C13

Infiltration temperature (°C)	Infiltration pressure (MPa)	Density (g/cm^3)	Theoretical density (%)	Bending strength (MPa)
650	1	1.78	63.5	70 ± 22
650	2	2.05	72.8	110 ± 21
650	3	2.27	80.9	163 ± 19
700	1	2.38	84.8	177 ± 20
700	2	2.55	90.7	264 ± 24
700	3	2.65	94.3	367 ± 22
750	1	2.60	92.6	295 ± 18
750	2	2.69	95.7	416 ± 23
750	3	2.75	97.8	518 ± 15
800	1	2.71	96.5	465 ± 17
800	2	2.77	98.5	533 ± 16
800	3	2.78	99.1	558 ± 14

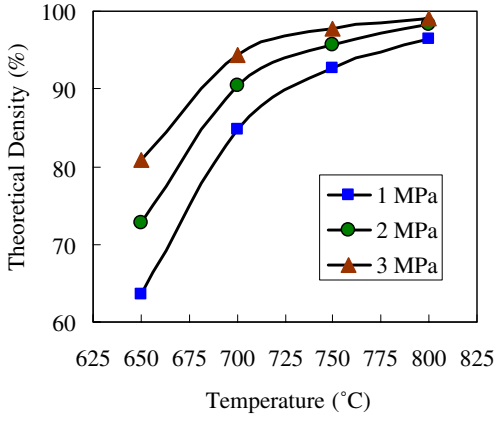

Fig. 2. Theoretical density increase versus infiltration temperature and pressure.

early solidification or congestion before infiltration is completed.

Scanning electron microscope image analysis of the infiltrated composite samples was made. The samples were polished and etched with Kellers solution before examination. As shown in Fig. 3(a) and (b), the infiltration of the highly porous Al_2O_3/SiC preform (sample C13) has been successfully achieved by the Al–Si–Mg alloy at 750 °C for 3 MPa. This confirms that the applied gas pressure is sufficient to overcome the surface tension between liquid Al and Al_2O_3/SiC ceramic preform. The honeycomb structure of the preform is clearly shown in these composite samples. The high and low magnification of the composites shows that the matrix alloy is penetrated all around the preform. Negligible residual porosity is left within the composites not only because of infiltration condition, also because of micro shrinkage between the dendrite arms. Some post-heat treatment may be needed to improve matrix properties. Moreover, uniform incorporation of SiCp and flaky alumina within the pore walls is clearly visible in Fig. 3(b). That is to say the pore walls are themselves ceramic composites which can combine both ceramic properties as reinforcement. During SEM examination, EDS analysis was also taken from the composites surface and the peaks, shown in Fig. 4, were obtained. While oxygen peak confirms the presence of alumina, carbon peaks confirms the presence of SiCp within the composite structure. Therefore, these SEM structures are evidence of successful incorporation of dual ceramic (Al_2O_3/SiC)-reinforced Al matrix composites via gas pressure infiltration.

3.2. Fracture behaviour

Bending test results are shown in Table 2 and Figs. 5–7. Bending tests were carried out for all dual particles (Al_2O_3/SiC) containing Al matrix composite samples,

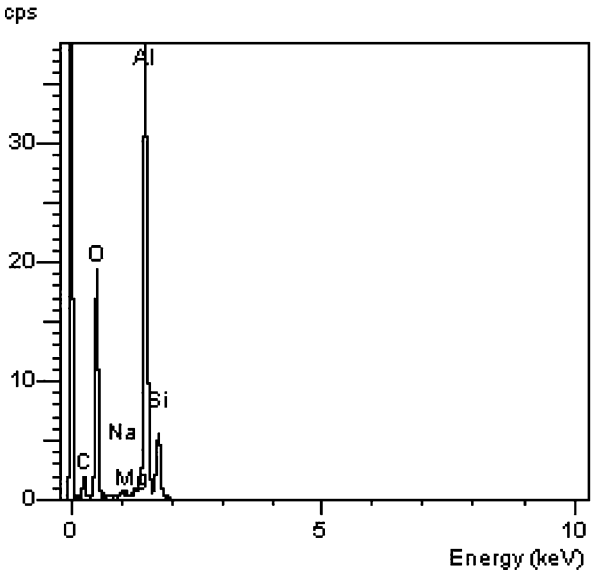

Fig. 4. EDS analysis of infiltrated composite.

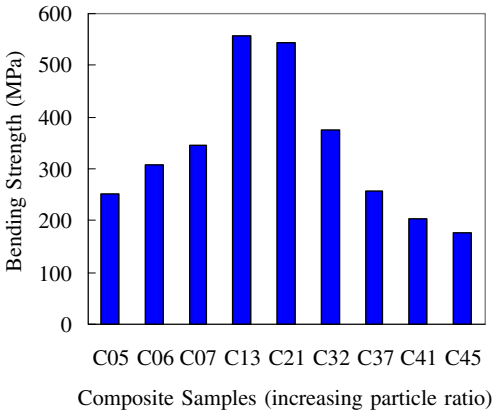

Fig. 5. Effect of particle rate on bending strength.

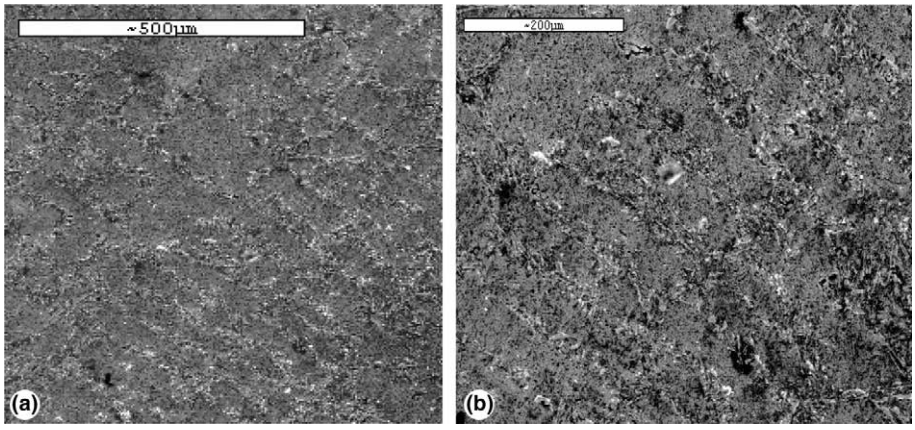

Fig. 3. SEM images of the Al_2O_3/SiCp-reinforced Al matrix composites: (a) low and (b) high magnification of sample C13.

which infiltrated at 800 °C and 3 MPa pressure. The results are plotted in Fig. 5. As shown in Fig. 5, the strength values fluctuate as the reinforcing particle ratio is increased. The lower and higher particle reinforcements of Al matrix result in low bending strength values. Highest strength value is achieved for the sample C13 which contains 13 vol% reinforcement phase. For the lower particle reinforcements, the particle ratio is not sufficient to prevent composite failure at higher loads since propagating cracks cannot be hindered by sufficient particles. On the other hand, for the higher particle reinforcements, particle contacts increased and therefore liquid Al is not able to enter all inter-particles which cause matrix free regions. This results in significant amount of porosity and undesired particle contacts in the resulting composites. During failure, cracks easily initiate and propagate in this region which deteriorates composite property. For a successful reinforcement, load must transfer from matrix to particle so that reinforcement can be carried out. This is not obtained when high ratio of particle-reinforced composite is fractured, since the particles are not wholly grabbed by the matrix. Hence, optimum particle ratio has been determined between 13 and 21 vol% to achieve highest strength values.

Since maximum strength was obtained for the sample C13 at 800 °C for 3 MPa pressure, the other lower pressure and temperature infiltrations were carried out only for the sample C13. When all figures and tables are examined, it can be seen that there is a relation between bending strength and infiltration temperature and pressure. The highest strength value, which can be obtained, is 558 MPa for 800 °C infiltration temperature and 3 MPa gas pressure. This value is quite high compared with unreinforced Al–Si alloy. However, there are no significant strength differences for the constant temperature at 800 °C, the strength values have only changed by 465, 530 and 558 MPa even though the pressure is increased threefold by 1, 2 and 3 MPa gas pressure, respectively. Since high temperature has reduced viscosity and increased wettability, pressure increase has not changed much relative density and dependence on bending strength. Bending strength is sensitive to the relative density, which is dependent on residual porosity in composite samples. Therefore, the denser the sample the higher strength value can be obtained. The residual porosity can be occurred by several reasons such as non-wetting, sufficient temperature and pressure, close porosity in the preform and micro shrinkage after solidification.

Figs. 6 and 7 show three point bending results for the sample C13. As the infiltration temperatures and pressures increased, strength values also increased. The samples produced at 650 °C exhibited very low level strengths, and minimum strength variations were observed for each pressure (Fig. 6) although maximum

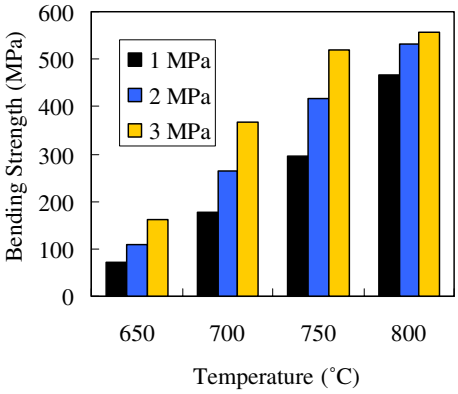

Fig. 6. Bending strength increase depending on infiltration temperature and pressure.

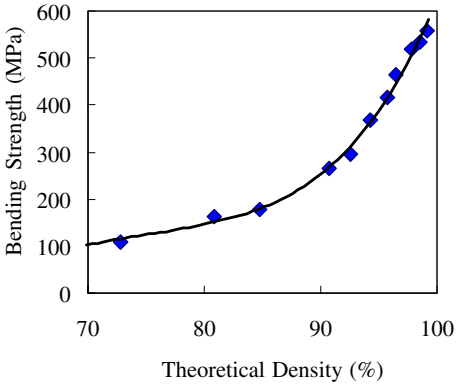

Fig. 7. Bending strength values as a function of theoretical density.

relative density differences occurred at 650° as shown in Fig. 2. Same narrow strength variations have been observed for 800 °C infiltrations for different pressures although relative densities are very close to each other. The slight density differences result in significant strength differences for the high temperature infiltrated samples, since the strength is very sensitive to residual porosity. For higher porosity, same sensitivity to relative densities has not been observed for the sample produced at low temperatures and pressures. This situation is clearly shown in Fig. 7. While gradual strength increase occurs below 90% TD, sharp strength increase is observed over 90% TD. This reveals that as the density of the MMCs approaches TD, enormous strength increase can be observed.

When fracture surface of the sample C13 is observed in Fig. 8, it can be concluded that dual particle (Al_2O_3/SiC) reinforcement of Al matrix composite played an important role during fracture. The combination of flaky alumina grains and encapsulated SiC particles provides crack hindering and deflection. Soft nature of Al matrix becomes rigid when it is reinforced with these particles and because of the fact that elastic modulus

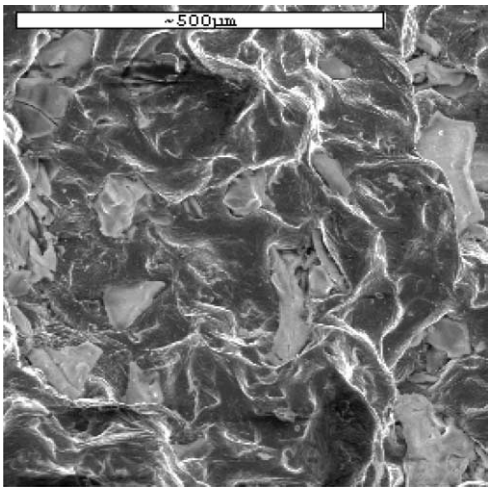

Fig. 8. Fracture surface of infiltrated composites.

increases. This rigidity lowers initial displacement and increase strength and elastic modulus. Two factors can lead to lower the effectiveness of reinforcement. One is the serious interfacial reactions between particles and matrix, which will cause the earlier failure of the particles. The other is the weakened interfacial bond between particles and matrix but without the damage of particles. The two cases correspond to the two kinds of fractographs with different characteristics, in the former one, the particles are easily fractured near the main crack plane. In the latter, since more particles will be pulled out from the matrix strength will decrease due to the low interfacial bond. And the pulled out particle lengths are longer. SEM fractography observation for the composites exhibited optimum interfacial bond giving the highest strength. This optimisation has been provided by tailoring of SiC and alumina. During fabrication of perform, alumina is coated on SiC particles and contributed fracture mechanism. Because of the composite stiffness, crack initiation is delayed and crack propagating is deflected by alumina particles first. If the crack is able to pass thorough alumina particles SiC particles can deflect the cracks because of interface between alumina and encapsulated SiC particles. In Fig. 8, the particles are uniformly distributed within the matrix and ductile fracture of matrix has been observed. Fracture surface is rough and some particle pull-out is visible. This shows that crack deflection occurred while crack is propagating and reinforcement is achieved.

The main properties of this preform is that it contains high porosity (up to 95 vol%) which leads to low particle reinforcement and it provides dual particle (Al_2O_3/SiC) reinforcement after aluminium infiltration. The incorporation of these two ceramic particles within the preform provided united reinforcement during failure of aluminium matrix composites. Furthermore, increasing SiC particles provided lower porosity which allowed higher particle reinforcement after infiltration. This means that particle/matrix ratio can be adjusted by changing the rate of SiC particles. Thus, the problem of low particle reinforcement in infiltration studies has been overcome, since production of highly porous preform is achieved. It is also possible to control the mechanical and physical properties of the composite for wide range of applications by changing particle/matrix ratio which is dependent on SiC particles.

4. Conclusion

High porous dual ceramic (Al_2O_3/SiC) preform was produced by chemical process for liquid aluminium infiltration and a gas pressure infiltration system was design to produce Al matrix composites. Increasing SiC in the preform lowered pore size and porosity and allowed to adjust particle/matrix ratio. Infiltration temperature and pressure are both effective for the infiltration but at low infiltration temperature high pressure is needed. Al–Si–Mg alloys can be infiltrated to this preform in spite of poor wetting properties. Bending behaviour of resulting composites exhibited high strength value. Maximum strength (558 MPa) was obtained for 13 vol% dual particle-reinforced Al matrix composites. The infiltration temperatures and pressures both increased relative density which influenced bending strength of the composites. Fracture surface of the composite showed that uniform particle distribution was obtained and reinforcement was achieved.

Acknowledgements

The authors acknowledge with sincere gratitude the financial support provided by the Turkish State Planning Organization (DPT) project 2000K150570.

References

[1] Alonso A, Paamies A, et al. Metal Trans A 1993;24:1423.
[2] Mubaraki B, Bandyopandhyay S, Fowle R, Mathew P. J Mater Sci 1995;30:6273–80.
[3] Taya M, Arsenault RJ. Metal matrix composites. Oxford: Pergamon Press; 1989. pp. 51–63.
[4] Schwartz MM. Composite materials handbook. New York: Mc Graw-Hill; 1984.
[5] Young-Ho S, Chung-Gil K. J Mater Process Technol 1995;55:370–9.
[6] Long S, Beffort O, Cayron C, Bonjour C. Mater Sci Eng A 1999;269:175–85.
[7] Chadwick GA. Mater Sci Eng A 1991;135:23–8.
[8] Long S, Zhang Z, Flower HM. Acta Metal Mater 1994;42:1389–97.

[9] Fletcher TR, Cornie JA, Russell KC. Mater Sci Eng A 1991;144:159–60.
[10] Garcia-Cordovilla C, Louis E, Narciso J. Acta Mater 1999;47:4461–79.
[11] Masur LJ, Mortensen A, Cornie JA, Flemings MC. Metall Trans A 1989;20:2549–57.
[12] Nourbakhsh S, Margolin H, Liang FL. Metall Trans A 1989;20(10):2159–66.
[13] Chu S, Wu R. Comp Sci Technol 1999;59:157–62.
[14] Pacewesca B. Therm Acta 1992;200:387–400.
[15] Altinkok N, Demir A, Ozsert I. Composites Part A: Appl Sci Eng 2003;34:577–82.
[16] ASTM B-312. Standard test method for green strength for compacted metal powder specimens. Annual book of ASTM standards; 1996. p. 02.05.